

# Cassini Maneuver Experience for the Fourth Year of the Solstice Mission

Mar Vaquero\*, Yungsun Hahn, Paul Stumpf, Powtawche Valerino,  
Sean Wagner, and Mau Wong†

After sixteen years of successful mission operations and invaluable scientific discoveries, the Cassini orbiter continues to tour Saturn on the most complex gravity-assist trajectory ever flown. To ensure that the end-of-mission target of September 2017 is achieved, propellant preservation is highly prioritized over maneuver cycle minimization. Thus, the maneuver decision process, which includes determining whether a maneuver is performed or canceled, designing a targeting strategy and selecting the engine for execution, is being continuously re-evaluated. This paper summarizes the maneuver experience throughout the fourth year of the Solstice Mission highlighting 27 maneuvers targeted to nine Titan flybys.

## Nomenclature

$\Delta V$	Change in velocity magnitude, km/s
$V_\infty$	Hyperbolic excess velocity vector, km/s
$X_{S/C}$	Spacecraft position element, km
$Y_{S/C}$	Spacecraft position element, km
$Z_{S/C}$	Spacecraft position element, km
$\mathbf{x}'\mathbf{y}'\mathbf{z}'$	Saturn-Titan rotating coordinate frame
$\mathbf{xyz}$	J2000 inertial coordinate frame
$\mathbf{X}_{S/C}$	x-axis, spacecraft inertial coordinate frame
$\mathbf{Y}_{S/C}$	y-axis, spacecraft inertial coordinate frame
$\mathbf{Z}_{S/C}$	z-axis, spacecraft inertial coordinate frame
$m$	Mass, kg
$\mathbf{B} \cdot \mathbf{R}$	Vertical axis of the B-plane, km
$\mathbf{B} \cdot \mathbf{T}$	Horizontal axis of the B-plane, km
$TCA$	Time of closest approach, seconds
$\Delta \mathbf{B} \cdot \mathbf{R}$	Change in vertical axis of the B-plane, km
$\Delta \mathbf{B} \cdot \mathbf{T}$	Change in horizontal axis of the B-plane, km
$\Delta TCA$	Change in time of closest approach, seconds
$TF$	Time-of-flight, seconds
$\Delta TF$	Change in time-of-flight, seconds

## I. Overview

LAUNCHED on October 15, 1997 to observe Saturn and its moons, rings, and magnetosphere, the Cassini-Huygens spacecraft successfully entered Saturn orbit on July 1, 2004 to begin its four-year Prime Mission.<sup>1</sup> Shortly after arriving at Saturn, the Huygens probe was released from the orbiter and landed on the surface of Titan. After four years of successful mission operations and invaluable scientific discoveries, two mission

---

\*Corresponding Author; *Mailing Address*: Jet Propulsion Laboratory, California Institute of Technology, Mail Stop 230-205, 4800 Oak Grove Drive, Pasadena, CA 91109-8099; *Tel*: (818) 354-5670; *Fax*: (818) 393-4215; *E-mail address*: Mar.Vaquero@jpl.nasa.gov

†Authors are members of the Flight Path Control Group and the Cassini Navigation Team, Jet Propulsion Laboratory, California Institute of Technology, Pasadena, CA 91109

extensions followed: the two-year Equinox Mission, beginning on September of 2008, and the seven-year Solstice Mission, starting on September of 2010. The Solstice Mission, designed to extend the mission lifetime past Saturn's northern summer solstice to increase the temporal baseline observable to two Saturnian seasons,<sup>2</sup> is comprised of 56 targeted flybys of Titan, 12 close Enceladus flybys (four of which pass through the water ice plume emanating from the south polar region), and five close flybys of Dione and Rhea with a total of 207 maneuver opportunities.<sup>2</sup> Altogether, the Cassini missions represent the most complex gravity-assist trajectory ever flown.<sup>1,2,3</sup> The entire Cassini Mission is proposed to end in 2017 with a series of 22 orbits each passing within a few thousand kilometers of the cloud tops of Saturn, and ultimately impacting Saturn.<sup>2</sup> With three more years planned for Cassini to fly the Saturn tour, the maneuver decision process is continuously re-evaluated as propellant preservation is now highly prioritized over maneuver cycle minimization. This decision process includes determining whether a maneuver is performed or canceled, deciding the maneuver design strategy, and choosing which engine to use for the maneuver, if executed. Generally, propellant savings are achieved by minimizing the  $\Delta V$  cost across several downstream maneuvers as opposed to canceling a maneuver. The propellant savings that result from not implementing a maneuver may add  $\Delta V$  to future maneuvers, resulting in an increased overall  $\Delta V$ .

Previous papers from the Cassini Navigation Team report on the maneuver experience during the Cassini orbiter interplanetary cruise to Saturn, the Prime and Equinox Missions, as well as the first three years of the Solstice Mission.<sup>4, 5, 6, 7, 8, 9, 10, 11, 12, 13, 14, 15</sup> This paper focuses on the maneuver activities of the Cassini spacecraft from July 30, 2013 through June 15, 2014, including 27 planned Orbit Trim Maneuvers (OTMs) and spanning the fourth year of the Solstice Mission. To maintain the prescribed trajectory or to preserve downstream  $\Delta V$ , 21 of the 27 maneuvers (78%) were performed. The planned maneuvers in the fourth year of the Solstice Mission, OTM-356 through OTM-382, were designed to achieve nine targeted flybys of Titan (T94–T102). These nine encounters are part of the second inclined phase (**In-2**) of the Solstice Mission. From May 2013 through May 2014, a series of resonant and generally longer period orbits (most  $> 32$  days) are exploited to reduce the trajectory inclination from  $61.7^\circ$  to  $40.7^\circ$ . This phase of the mission, (**In-2**), provides both northern and southern hemisphere, low phase Titan surface coverage and multiple inclined passages through Saturn's magnetotail region.<sup>2</sup> Generally, the geometry of each targeted flyby is driven by a particular science objective. Such science drivers during this time frame include acquisition of images of two of the largest lakes on Titan, Ligeia Mare and Punga Mare, analysis of the effects of the solar input on Titan's atmosphere, and monitoring of the evolution of the cloud system over the North Pole as Titan summer approaches.<sup>2</sup> Starting in May 2014, the T101–T103 flybys increase inclination, rather than continue to decrease it as in the prior sub-phase, in order to achieve three Radio Science Subsystem (RSS) and Ultraviolet Imaging Spectrograph (UVIS) Titan occultations for atmospheric studies of Titan's polar regions.<sup>16</sup> The first two of these three Titan flybys encounters, T101 and T102, are discussed in this paper.

The spacecraft trajectory from July 2013 to June 2014, as viewed from Saturn's north pole with the Sun direction along the horizontal axis, is depicted in the petal plot in Figure 1. The time profile of orbital inclination and orbital period, from which it is possible to determine the orbital effect of each flyby, is represented in Figure 3. Additionally, an orbital events diagram appears in Figure 5 to provide the context of how each maneuver relates to the targeted encounters.<sup>17</sup> Each maneuver and encounter in the scope of this paper is presented as a function of true anomaly, with each row representing one spacecraft revolution around Saturn measured from apocrone (Saturn apoapsis) to apocrone. Maneuvers are color-coded as either executed (blue) or canceled (yellow). Each revolution around Saturn is numbered, and its anomalistic period is listed in days (time elapsed between two consecutive passes through apoapsis). One revolution spans  $360^\circ$  of true anomaly (the horizontal axis), negative from apoapsis ( $180^\circ$ ) to periapsis ( $0^\circ$ ), and positive from periapsis to apoapsis.

To address the end-of-mission date in 2017 and a dwindling propellant supply, the Cassini Project has modified its rationale for maneuver implementations and cancelations. Earlier in the mission, the reduction of maneuver cycles was a prime concern because propellant reserves were high. Now that Cassini is in its final extended mission, concerns have shifted towards propellant preservation. However, reducing the Reaction Control Subsystem (RCS) usage to help safeguard its functionality is still important, as RCS is needed for attitude control, pointing Cassini's high-gain antenna to Earth for communication, and reaction wheel management. The balance of both is, therefore, the main driver of the current navigation strategy.

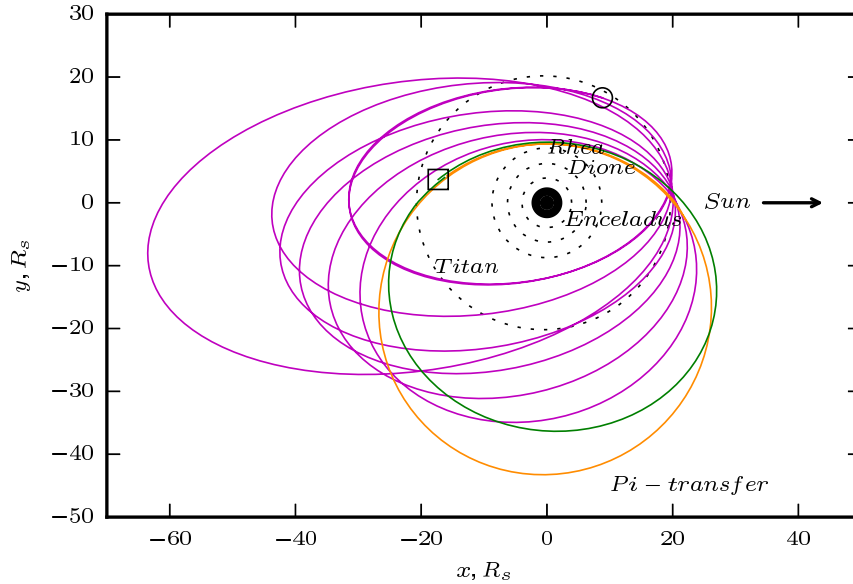


Figure 1: Saturn North Polar View (Sun-Fixed)

Figure 2: Cassini's trajectory from 26-Jul-2013 (circle) to 18-Jun-2014 (square) as viewed from Saturn's north pole, and outlining the orbits of Titan, Enceladus, Dione, and Rhea; Saturn and the rings are shown to scale, **In-2B** trajectory from 23-May-2013 to 07-Apr-2014 (purple), the T100–T101 pi-transfer from 07-Apr-2014 to 17-May-2014 (orange), start of **In-2C** trajectory from 17-May-2014 to 18-Jun-2014 (green). The Sun is to the right of the diagram and the unit distance is  $R_s = 60,330$  km (the equatorial radius of Saturn at 0.1 bar atmospheric pressure.)

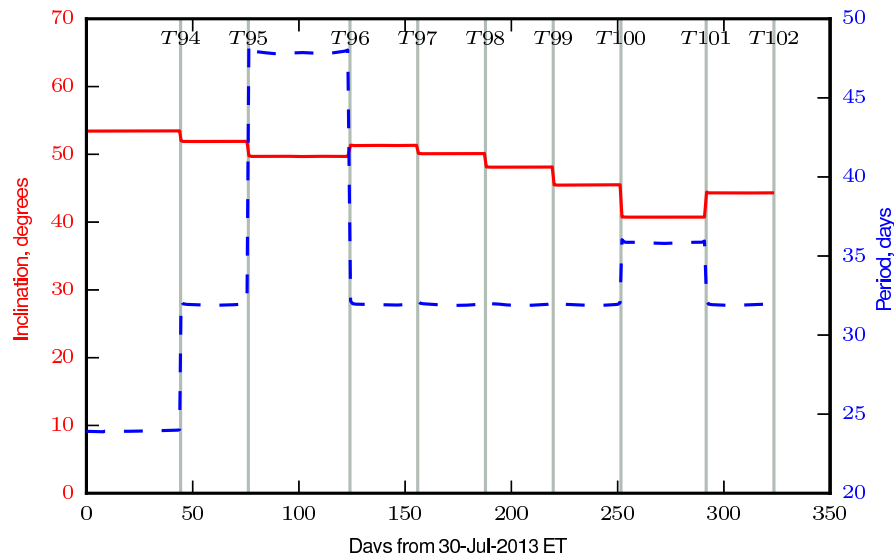


Figure 3: Inclination and Orbital Period

Figure 4: Instantaneous orbital inclination with respect to Saturn's true equator (solid line, left axis) and orbital period (dotted line; right axis). Encounters are labeled to highlight the effect of each flyby on the orbital parameters.

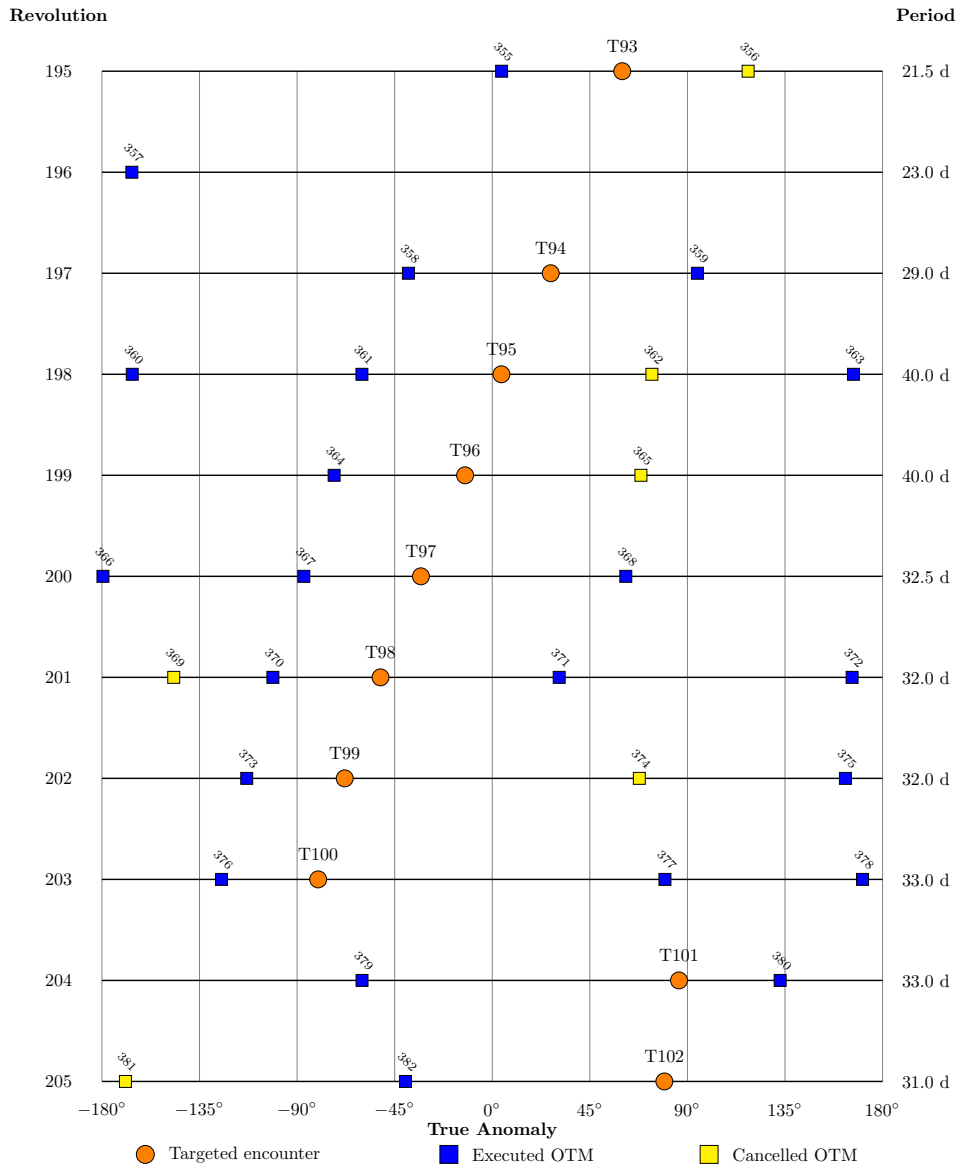


Figure 5: Titan-93 – Titan-102 Orbital Events

## II. Navigation Strategy

The Cassini spacecraft takes advantage of the substantial gravity assists provided by each Titan encounter. For example, a Titan flyby at an altitude of 1,000 km and a  $V_\infty$  of 5.5 km/s supplies about 840 m/s of  $\Delta V$  to Cassini, and lower-altitude flybys impart even more. The maneuvers executed by Cassini are dwarfed in comparison. For reference, about 98% of the total  $\Delta V$  required by the entire mission is provided by Titan alone. The nominal navigation strategy consists of scheduling three orbit trim maneuvers between each targeted encounter, as illustrated in Figure 6 for an outbound-to-inbound leg. Note that an outbound flyby occurs after pericrone (Saturn periapsis) whereas an inbound encounter occurs before pericrone. A cleanup maneuver, about three days after an encounter, removes the orbital dispersion errors incurred by inaccuracies in the flyby conditions; a shaping maneuver, normally located near apoapsis, targets the encounter conditions; and an approach maneuver, about three days before an encounter, refines the orbit before an encounter, if necessary.

Maneuvers are performed by Cassini's bipropellant Main Engine Assembly (MEA) or monopropellant Reaction Control Subsystem (RCS) (see Figure 7). The reaction control subsystem, which is used for

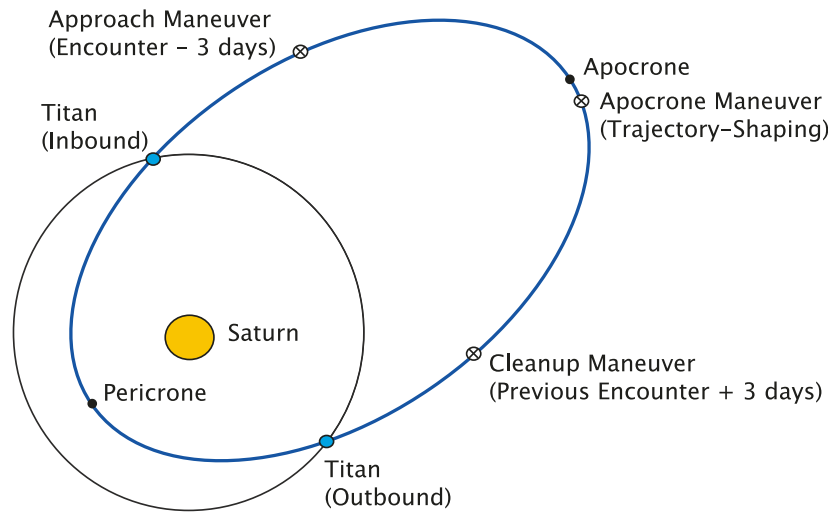


Figure 6: Navigation Strategy of Three Maneuvers per Flyby for Saturn Tour

attitude control, high-gain antenna pointing for communication, reaction wheel momentum dumps, and small maneuvers ( $\Delta V < 0.25$  m/s), consists of four hydrazine thruster clusters grouped into two sets: the first set is along  $\pm \mathbf{Y}_{S/C}$ , and is used to make balanced roll turns about the  $\mathbf{Z}_{S/C}$  axis; the second set faces the  $-\mathbf{Z}_{S/C}$  axis and is used to make unbalanced yaw turns about the  $\mathbf{Y}_{S/C}$  axis. The main engine assembly is employed for larger burns if the predicted burn time is at least 1.5 sec (actual burn time  $> 1.3$  sec). This burn duration minimum was set in the past to avoid a software limitation of 1 sec for burn times.<sup>14</sup> Currently, this translates to MEA burns that are at least 0.25 m/s. The first two maneuvers are usually deterministic and optimized together in a chained two-impulse optimization strategy,<sup>18</sup> which minimizes total deterministic  $\Delta V$  across several encounters while controlling asymptote errors without altering downstream flyby aim points after each encounter. The three orbit trim maneuvers are targeted to the upcoming encounter's three B-plane<sup>19</sup> flyby conditions: the spatial components  $\mathbf{B} \cdot \mathbf{R}$  and  $\mathbf{B} \cdot \mathbf{T}$ , and the time of flight, TF. These targets were determined during the mission design phase and are defined in the reference trajectory, which provides predetermined maneuver locations and flyby targets according to science sequence planning and objectives.

Each maneuver is executed in a turn-and-burn manner, that is, the required burn attitude is achieved by performing a roll turn followed by a yaw turn (wind turns), the burn is then executed and, after completion, the turns are reversed to return to the original attitude (unwind turns). Turns performed with the Reaction Wheel Assembly (RWA) and roll turns performed by the RCS do not impart  $\Delta V$  to the spacecraft. Moreover, yaw turns executed by RCS do contribute  $\Delta V$  because these thrusters are unbalanced about the  $\mathbf{Y}_{S/C}$  axis. All roll turns and the yaw turn for RCS maneuvers are typically executed by the RWA. However, the yaw turn for MEA maneuvers is usually performed by RCS thrusters. For this reason, the computation of MEA maneuvers needs to account for the  $\Delta V$  imparted by the turns. Gates models<sup>20</sup> of the maneuver execution errors are implemented for statistical analysis, a priori estimates for OD maneuver reconstructions, determination of maneuver delivery accuracies, and maneuver performance assessments.<sup>21</sup> The execution-error models have been updated periodically based on maneuver performance during the Saturn tour.<sup>21,22</sup> For reference, the execution-error models employed by Cassini since August 2012 are summarized in the Table 1.

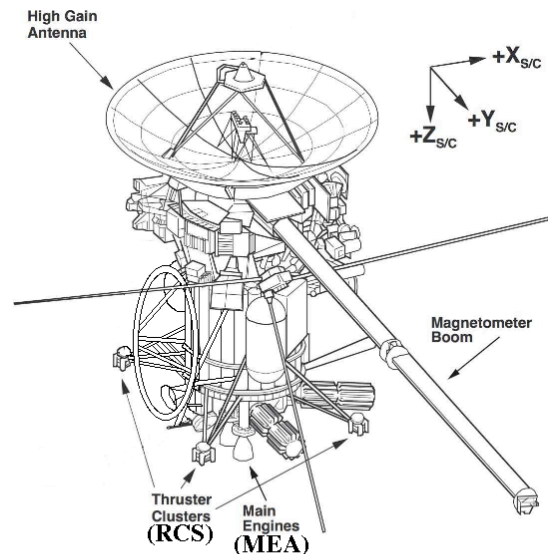


Figure 7: Cassini Orbiter

Table 1: 2012-1 Execution-Error Models ( $1\text{-}\sigma$ ). Valid for MEA burns  $\leq 13$  m/s and RCS burns  $\leq 0.3$  m/s.

		MEA	RCS
Magnitude	Proportional (%)	0.02	0.4
	Fixed (mm/s)	3.5	0.5
Pointing (per axis)	Proportional (mrad)	1.0	4.5
	Fixed (mm/s)	5.0	0

A planned maneuver can be canceled if it is determined that its execution will not improve encounter conditions, yield downstream  $\Delta V$  savings, or if a subsequent maneuver can attain the encounter conditions at a lower  $\Delta V$  cost. For instance, a common cancellation case is an approach maneuver preceded by accurate shaping maneuvers. Regardless, these criteria are subordinate to science requirements.<sup>18</sup> Depending on science prerequisites, certain encounters admit the modification of targeting parameters. Such modification can be necessary for two reasons: (1) when a maneuver is smaller than the smallest implementable maneuver (approximately 10 mm/s), it is possible to modify the encounter time by a few tenths-of-a-second and artificially increase the maneuver magnitude and (2) some target modifications to the spatial components  $\mathbf{B} \cdot \mathbf{R}$  and  $\mathbf{B} \cdot \mathbf{T}$  can yield downstream  $\Delta V$  savings (about 1 gram of hydrazine per mm/s saved for RCS-sized maneuvers). Both of these situations were encountered during the fourth year of the Solstice Mission.

### III. Operations During the Magnetotail Passage: July 2013 – June 2014

From July 2013 through June 2014, a series of generally longer-period ( $> 32$  days) resonant Titan-to-Titan transfers (T92–T102), targeted by OTMs 353–382, decreased the trajectory inclination by  $20^\circ$ , that is, from  $61.7^\circ$  to  $40.7^\circ$ , during the middle portion of the second inclined phase. This second phase provides both northern and southern hemisphere, low phase Titan surface coverage and multiple inclined passages through Saturn’s magnetotail region.<sup>2</sup> Highlights of the transfers and maneuvers planned during this time frame are summarized.

#### A. Reconstruction of Maneuvers and Targeted Flybys

The maneuver design and reconstruction history from July 30, 2013 through June 15, 2014, covering OTMs 356–382, is presented in Table 2. The table lists the maneuver epoch, true anomaly, central angle, design and reconstructed  $\Delta V$ s (magnitude, right ascension, and declination), and engine type (main engine or RCS). The reported true anomaly corresponds to the instantaneous Saturn-centered orbit at burn time. The central angle is defined by the three-dimensional angle between the position vectors at the burn time and encounter (counting multiple revolutions). Maneuvers are grouped by the corresponding targeted encounters; the shaded rows contain the encounter name, time of closest approach, flyby altitude, flyby  $\Delta V$  imparted to spacecraft, whether the flyby is inbound (before pericrone) or outbound (after pericrone), days to next encounter, and whether the target time is modified. Out of 27 opportunities (OTMs 356–382), 21 maneuvers were performed, five of which were implemented with MEA and 16 with RCS.

The  $\Delta V$  characteristics of each maneuver covered in the scope of this paper are listed in Table 3, including the maneuver location (true anomaly and central angle), the  $\Delta V$  magnitude, the roll and yaw turn angles for burn orientation, and the burn durations. Each maneuver has both prime and backup designs. Backup maneuver windows are scheduled approximately 24 hours after the prime maneuver windows. Data from executed maneuvers are shaded in gray, and data from main engine maneuver designs are indicated in bold.

The targeted encounter conditions, defined in the 110818 reference trajectory, and the reconstructed flyby differences for each of the 10 flybys from T93 to T102, three of which had modified targets (T94, T96, and T101), are provided in Table 4. Recall that the reference trajectory provides predetermined maneuver locations and flyby targets according to science sequence planning and objectives; 110818 is the release date of the reference trajectory update (August 18, 2011). For reference, the total number of intentionally altered flybys up to date in the Solstice Mission is 14, as compared to the Prime and Equinox Missions total of 6.

Table 2: Maneuver History (OTMs 355–382)

Maneuver	Orbit Location	Maneuver Time (UTC SCET)	True Anomaly (deg)	Central Angle (deg)	Total Design $\Delta V^*$			Total Reconstructed $\Delta V^*$			Burn Type
					Mag. (m/s)	RA (deg)	Dec. (deg)	Mag. (m/s)	RA (deg)	Dec. (deg)	
OTM-355	T93–3d	23-Jul-2013 08:24	4.32	97.16	0.072	280.57	50.18	0.071	279.91	50.24	RCS
<i>Titan-93 (T93): 26-Jul-2013 11:57:29 ET, Alt.= 1400 km, Flyby <math>\Delta V= 771.5</math> m/s, 47.8 days to T94</i>											
OTM-356	T93+4d	30-Jul-2013 07:53	118.01	650.76	..... CANCELLED .....						
OTM-357	~apo	07-Aug-2013 07:22	-166.29	575.18	3.614	288.15	53.00	3.620	288.47	53.12	MEA
OTM-358†	T94–3d	09-Sep-2013 05:18	-38.65	87.61	0.035	151.83	-32.80	0.034	151.97	-32.93	RCS
<i>Titan-94 (T94): 12-Sep-2013 07:45:03 ET, Alt.= 1400 km, Flyby <math>\Delta V= 772.9</math> m/s, 31.9 days to T95, <math>\Delta(\mathbf{B} \cdot \mathbf{R}, \mathbf{B} \cdot \mathbf{T})=(+2.0, +3.0)</math> km</i>											
OTM-359	T94+4d	16-Sep-2013 04:47	94.62	282.59	0.033	43.38	20.72	0.032	43.73	20.79	RCS
OTM-360	~apo	30-Sep-2013 04:01	-166.02	183.31	0.071	123.83	-22.35	0.071	124.16	-22.62	RCS
OTM-361	T95–3d	11-Oct-2013 03:15	-60.10	77.49	0.019	125.13	-49.65	0.020	125.34	-49.70	RCS
<i>Titan-95 (T95): 14-Oct-2013 04:57:34 ET, Alt.= 961 km, Flyby <math>\Delta V= 860.5</math> m/s, 47.8 days to T96</i>											
OTM-362	T95+3d	17-Oct-2013 13:15	73.62	281.96	..... CANCELLED .....						
OTM-363	~apo	02-Nov-2013 12:15	166.57	189.05	0.364	331.36	50.10	0.365	331.61	50.65	MEA
OTM-364†	T96–3d	28-Nov-2013 00:45	-72.92	68.65	0.014	209.80	-42.22	0.014	209.96	-42.19	RCS
<i>Titan-96 (T96): 01-Dec-2013 00:42:26 ET, Alt.= 1400 km, Flyby <math>\Delta V= 772.1</math> m/s, 31.9 days to T97, <math>\Delta TF= -0.25</math> sec</i>											
OTM-365	T96+4d	04-Dec-2013 18:00	68.57	265.87	..... CANCELLED .....						
OTM-366	~apo	17-Dec-2013 23:32	-179.52	154.04	0.386	320.73	55.44	0.379	321.51	55.66	MEA
OTM-367	T97–3d	29-Dec-2013 22:48	-86.89	61.52	0.115	327.85	48.51	0.116	327.36	48.76	RCS
<i>Titan-97 (T97): 01-Jan-2014 22:00:48 ET, Alt.= 1400 km, Flyby <math>\Delta V= 772.5</math> m/s, 31.9 days to T98</i>											
OTM-368	T97+4d	05-Jan-2014 16:03	61.59	251.75	0.103	194.27	-37.36	0.103	194.67	-37.42	RCS
OTM-369	~apo	25-Jan-2014 14:51	-146.90	100.34	..... CANCELLED .....						
OTM-370	T98–3d	30-Jan-2014 20:51	-101.16	54.70	0.056	330.56	48.57	0.054	330.14	48.78	RCS
<i>Titan-98 (T98): 02-Feb-2014 19:13:45 ET, Alt.= 1236 km, Flyby <math>\Delta V= 803.3</math> m/s, 31.9 days to T99</i>											
OTM-371	T98+3d	05-Feb-2014 14:07	30.86	264.20	0.089	202.45	21.43	0.090	201.97	21.20	RCS
OTM-372	~apo	17-Feb-2014 13:24	165.98	129.21	1.683	13.75	25.67	1.681	13.79	25.73	MEA
OTM-373	T99–3d	03-Mar-2014 18:56	-113.23	48.46	0.024	344.51	33.78	0.024	344.29	33.88	RCS
<i>Titan-99 (T99): 06-Mar-2014 16:27:54 ET, Alt.= 1500 km, Flyby <math>\Delta V= 755.0</math> m/s, 31.9 days to T100</i>											
OTM-374	T99+4d	10-Mar-2014 12:12	67.82	212.95	..... CANCELLED .....						
OTM-375	~apo	20-Mar-2014 11:28	162.87	117.98	0.542	22.05	8.25	0.545	21.98	8.27	MEA
OTM-376‡	T100–3d	04-Apr-2014 10:29	-124.87	45.79	0.055	193.45	-29.46	0.054	193.66	-29.63	RCS
<i>Titan-100 (T100): 07-Apr-2014 13:42:21 ET, Alt.= 963 km, Flyby <math>\Delta V= 860.7</math> m/s, 40.1 days to T101</i>											
OTM-377‡	T100+4d	11-Apr-2014 10:00	79.64	371.13	0.037	105.70	-6.29	0.036	105.83	-6.55	RCS
OTM-378‡	~apo	24-Apr-2014 09:01	170.77	280.05	0.036	54.23	-2.69	0.036	54.17	-2.84	RCS
OTM-379†, ‡	T101–3d	14-May-2014 07:46	-60.05	150.89	0.023	142.15	56.82	0.021	142.55	56.73	RCS
<i>Titan-101 (T101): 17-May-2014 16:13:22 ET, Alt.= 2994 km, Flyby <math>\Delta V= 569.8</math> m/s, 31.9 days to T102, <math>\Delta(\mathbf{B} \cdot \mathbf{R}, \mathbf{B} \cdot \mathbf{T})=(+0.75, +2.5)</math> km</i>											
OTM-380‡	T101+4d	21-May-2014 07:16	132.77	313.54	0.020	151.90	31.22	0.020	152.16	31.03	RCS
OTM-381‡	~apo	03-Jun-2014 06:15	-169.17	255.53	..... CANCELLED .....						
OTM-382‡	T102–3d	15-Jun-2014 11:44	-40.01	126.42	0.027	259.70	35.86	0.028	259.46	35.78	RCS
<i>Titan-102 (T102): 18-Jun-2014 13:29:32 ET, Alt.= 3659 km, Flyby <math>\Delta V= 511.6</math> m/s, 31.9 days to T103</i>											

\* Total  $\Delta V$  is the sum of  $\Delta V$ s due to the burn, roll and yaw turns, the pointing-bias-fix turn for MEA burns, and the 5.8 mm/s deadband tightening for RCS burns. Expressed in Earth Mean Equator & Equinox of J2000.0 coordinates (EME2000).  
Mag. = magnitude, RA = right ascension, Dec. = declination.

† Target condition(s) changed via maneuver.

‡ Reported reconstructed  $\Delta V$  values are based on preliminary OD estimates.

Table 3: Maneuver Designs (OTMs 355–382). *Data from executed maneuvers are shaded in gray, and data from main engine maneuver designs are indicated in bold.*

OTM	Prime Maneuver Window						Backup Maneuver Window					
	True Anomaly (deg)	Central Angle (deg)	$\Delta V$ Mag. (m/s)	Roll Angle (deg)	Yaw Angle (deg)	Burn Time (sec)	True Anomaly (deg)	Central Angle (deg)	$\Delta V$ Mag. (m/s)	Roll Angle (deg)	Yaw Angle (deg)	Burn Time (sec)
355	4.32	97.16	0.0721	-16.97	-95.71	66.34	40.97	60.49	0.1063	-15.59	-86.18	100.19
356	118.01	650.76	0.0733	164.86	-63.88	67.49	130.01	638.77	0.0898	169.74	-62.75	83.78
357	<b>-166.29</b>	<b>575.18</b>	<b>3.6145</b>	<b>-146.05</b>	<b>-87.69</b>	<b>20.70</b>	<b>-157.50</b>	<b>566.38</b>	<b>3.6033</b>	<b>-145.17</b>	<b>-96.32</b>	<b>20.64</b>
358	-38.65	87.61	0.0346	-101.22	-118.00	29.04	-10.43	59.37	0.0593	-96.53	-126.28	53.53
359	94.62	282.59	0.0331	-4.65	-10.68	27.55	106.94	270.28	0.0377	60.05	-12.88	32.10
360	-166.02	183.31	0.0714	17.15	-90.97	65.48	-160.28	177.57	0.0834	78.13	-83.38	77.36
361	-60.10	77.49	0.0185	-76.67	-97.29	13.10	-37.76	55.14	0.0282	-77.13	-106.00	22.69
362	73.62	281.96	0.0135	-159.66	-94.20	8.12	87.88	267.70	0.0131	-155.92	-93.69	7.72
363	<b>166.57</b>	<b>189.05</b>	<b>0.3642</b>	<b>144.41</b>	<b>-64.68</b>	<b>2.15</b>	<b>169.46</b>	<b>186.16</b>	<b>0.3509</b>	<b>145.69</b>	<b>-68.55</b>	<b>2.07</b>
364*	-72.92	68.65	0.0140	-50.28	-149.62	8.57	-54.56	50.28	0.0197	-100.56	-155.95	14.37
365	68.57	265.87	0.0265	3.92	-138.35	21.23	85.51	248.93	0.0339	-12.12	-126.54	28.62
366	<b>-179.52</b>	<b>154.04</b>	<b>0.3859</b>	<b>-144.70</b>	<b>-73.17</b>	<b>2.29</b>	<b>-174.17</b>	<b>148.68</b>	<b>0.4319</b>	<b>-145.15</b>	<b>-78.60</b>	<b>2.56</b>
367	-86.89	61.52	0.1154	-146.04	-72.00	109.73	-70.09	44.73	0.1856	-147.68	-62.63	179.40
368	61.59	251.75	0.1033	98.47	-142.76	97.56	81.47	231.86	0.1187	89.24	-155.05	112.78
369	-146.90	100.34	0.0161	-131.84	-106.00	10.68	-140.34	93.81	0.0191	-133.19	-102.54	13.70
370	-101.16	54.70	0.0558	-139.63	-71.40	50.46	-86.67	40.22	0.0863	-141.24	-66.37	80.73
371	30.86	264.20	0.0891	1.53	-133.21	83.70	61.51	233.54	0.2004	-5.46	-100.10	194.30
372	<b>165.98</b>	<b>129.21</b>	<b>1.6829</b>	<b>-167.76</b>	<b>-33.21</b>	<b>9.69</b>	<b>170.56</b>	<b>124.63</b>	<b>1.7239</b>	<b>-164.58</b>	<b>-37.07</b>	<b>9.93</b>
373	-113.23	48.46	0.0242	-167.74	-62.03	18.95	-100.69	35.93	0.0408	-169.26	-53.84	35.66
374	67.82	212.95	0.0037	4.53	-108.75	4.09	91.39	189.38	0.0050	-0.48	-90.16	5.41
375	<b>162.87</b>	<b>117.98</b>	<b>0.5420</b>	<b>160.41</b>	<b>-26.61</b>	<b>3.17</b>	<b>167.09</b>	<b>113.77</b>	<b>0.5384</b>	<b>166.24</b>	<b>-28.40</b>	<b>3.15</b>
376	-124.87	45.79	0.0549	19.86	-143.42	49.76	-114.58	35.50	0.0824	17.69	-144.36	77.37
377	79.64	371.13	0.0373	-158.38	-59.32	32.22	101.45	349.32	0.0480	-166.85	-66.04	42.96
378	170.77	280.05	0.0362	-46.48	-18.84	31.12	173.71	277.11	0.0346	-41.74	-16.63	29.46
379	-60.05	150.89	0.0228	-8.09	-79.64	17.61	-10.01	100.84	0.0157	-28.04	-81.01	10.45
380	132.77	313.54	0.0200	-165.63	-94.21	14.75	139.81	306.51	0.0169	-160.63	-94.08	11.63
381	-169.17	255.53	0.0005	-45.84	-151.23	0.82	-165.22	251.59	0.0006	-50.63	-152.21	0.90
382	-40.01	126.42	0.0272	-73.18	-120.01	22.14	9.75	76.65	0.0432	-81.80	-105.45	38.34

\* Prime maneuver design required a time-of-flight modification to make implementable.

Table 4: Targeted Encounter History (Titan-93 to Titan-102)

Encounter	Flyby Characteristics				Reference Trajectory Target Conditions (Earth Mean Orbital Plane & Equinox of J2000.0)				Flyby Differences from Reference Trajectory		
	In/ Out*	$V_\infty$ (km/s)	Period (days)	Inc. (deg)	<b>B·R</b> (km)	<b>B·T</b> (km)	TCA (ET SCET)	Alt.† (km)	$\Delta\mathbf{B}\cdot\mathbf{R}$ (km)	$\Delta\mathbf{B}\cdot\mathbf{T}$ (km)	$\Delta\text{TCA}$ (sec)
Titan-93	Out	5.44	23.9	53.4	-3529.87	-2398.45	26-Jul-2013 11:57:29	1400	0.39	0.38	0.04
Titan-94‡	Out	5.43	31.9	51.9	-741.84	-4203.28	12-Sep-2013 07:45:03	1400	1.89 (+2.0)	2.92 (+3.0)	0.02
Titan-95	Out	5.43	47.9	49.7	219.27	-3821.68	14-Oct-2013 04:57:34	961	0.11	0.17	-0.04
Titan-96‡	In	5.43	32.0	51.3	4198.46	-767.96	01-Dec-2013 00:42:26	1400	0.06	-0.007	-0.24 (-0.25)
Titan-97	In	5.43	32.0	50.1	3250.83	-2766.13	01-Jan-2014 22:00:48	1400	-0.17	-0.12	0.03
Titan-98	In	5.43	32.0	48.1	3409.29	-2283.90	02-Feb-2014 19:13:45	1236	0.13	0.42	-0.04
Titan-99	In	5.43	32.0	45.5	3841.06	-2081.48	06-Mar-2014 16:27:54	1500	-0.18	0.15	0.01
Titan-100§	In	5.43	35.9	40.7	3207.94	-2093.17	07-Apr-2014 13:42:21	963	0.23	-0.35	-0.01
Titan-101‡,§	Out	5.36	31.9	44.3	2128.65	-5473.63	17-May-2014 16:13:22	2994	0.82 (+0.75)	2.54 (+2.5)	-0.007
Titan-102§	Out	5.36	31.9	46.5	2802.59	-5907.25	18-Jun-2014 13:29:32	3659	-0.29	-0.13	-0.04

\* An inbound encounter occurs before pericrone (Saturn periapsis). An outbound flyby occurs after pericrone.

† Flyby altitudes not explicitly targeted by maneuvers; reported altitudes from reference trajectory (relative to a sphere).

‡ Target condition(s) changed via maneuver; the quantities in parentheses denote differences from the reference trajectory.

§ Reported flyby differences are based on preliminary orbit determination estimates.

## B. Resonant and pi- Transfers

Resonant orbits are a key element in the design of planetary and satellite flybys and powerful transfer mechanisms between orbits, significantly reducing the maneuver cost associated with transferring from one orbit to another. In a Titan-to-Titan  $n:m$  resonant transfer, the time-of-flight is an integer multiple of Titan’s period, where  $m$  represents the number of spacecraft orbits around Saturn and  $n$  is the number of Titan revolutions.<sup>23</sup> Consequently, the flybys at the beginning and end of a resonant transfer occur at approximately the same place in Titan’s orbit. The longitude of the encounters occurs on a fixed line passing from Saturn to Titan and the resonant transfer may be inclined. A total of nine Titan-to-Titan encounters span the time frame from July 2013 to June 2014; eight out of the nine transfer trajectories involve some form of resonance with Titan. These trajectories along with highlights of the corresponding orbit trim maneuver designs are summarized.

### 1. Titan-93 to Titan-94: 3:2 Resonant Transfer

Cassini’s 3:2 resonant trajectory from T93 on 26-July-2013 (blue dot) to T94 on 12-Sep-2013 is represented in Figure 8. The plot in Figure 8a depicts the trajectory as viewed from a Saturn-centered J2000 coordinate frame. For reference, the orbit of Titan is outlined and represented by the dotted magenta line. The black dots along the transfer orbit represent the location of the planned OTMs for the T93-T94 encounter and the blue/magenta arrows indicate the direction of motion of the spacecraft/Titan. Additionally, Cassini’s 3:2 resonant trajectory appears in Figure 8b as viewed from a Saturn-Titan rotating coordinate frame fixed at the center of the inertial coordinate frame, i.e., Saturn. The  $x'$ -axis of the additional rotating frame is always parallel to the line connecting the two primary bodies, Saturn and Titan, and directed from the largest (at the origin) to the smallest (at the right). The  $z'$ -axis is parallel to the orbital angular momentum vector associated with the motion of the system. Then,  $y'$  completes the right-handed vector basis. This rotating reference frame is standard for the well-know circular restricted three-body model. The stationary location of Titan ( $a_T, 0, 0$ ), as viewed in the rotating frame, is labeled in the Figure. Resonant orbits viewed from the perspective of a rotating frame offer valuable insight since the relationship between the resonance and

the frequency of conjunctions with Titan is more apparent. A special feature of resonant orbits only visible from a rotating frame perspective is the formations of 'loops', which indicate the passage of the spacecraft through an apse location. Consequently, the number of loops in a resonant transfer determines the integer  $n$  in an  $n:m$  resonant ratio. Resonant transfers are also categorized based on this ratio: exterior resonant orbits have a  $n:m$  ratio such that  $n > m$  whereas the ratio in interior resonances is such that  $n < m$ .

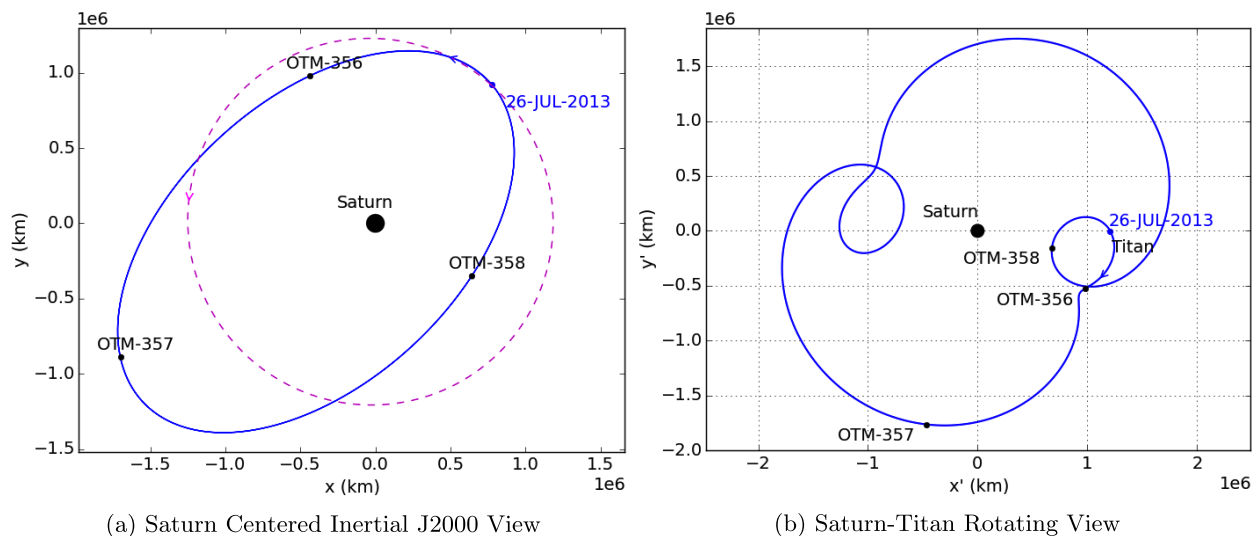


Figure 8: Cassini's 3:2 resonant trajectory from 26-July-2013 to 12-Sep-2013 as viewed from (a) inertial and (b) rotating reference frames.

The T94 encounter was targeted by OTMs 356–358. The small target miss at T93 resulted in a cancellation of the cleanup maneuver OTM-356. The subsequent apoapsis maneuver, OTM-357, was performed nominally as a main engine burn at 3.6 m/s, with the distinction of being the largest burn during the fourth year of the Solstice Mission. The approach maneuver to T94, OTM-358, was required to avoid a cancellation cost of 0.46 m/s and OTM-362 increasing to a borderline main engine burn of  $\sim 0.4$  m/s.

By altering the T94 aimpoint by +2 km in  $\mathbf{B} \cdot \mathbf{R}$  and +3 km in  $\mathbf{B} \cdot \mathbf{T}$  via OTM-358, an additional 0.17 m/s downstream  $\Delta V$  was saved (see Figure 9). For an explanation of how each contour plot was produced, see Reference 24.

## 2. Titan-94 to Titan 95: 2:1 Resonant Transfer

Cassini's 2:1 resonant trajectory from T94 on 12-Sep-2013 (blue dot) to T95 on 14-Oct-2013 is represented in Figure 10. The plot in Figure 10a depicts the trajectory as viewed from a Saturn-centered J2000 coordinate frame. The black dots along the transfer orbit represent the locations of the three planned maneuvers during this encounter: OTM-359, OTM-360, and OTM-361. Additionally, Cassini's transfer trajectory from T94 to T95 appears in Figure 10b as viewed from a Saturn-Titan rotating coordinate frame. The arrows indicate direction of motion. Note that this trajectory is highly inclined, but for visualization purposes, an  $xy$ -projection is presented.

Interestingly, performing either OTM-359 or OTM-360 only to target T95 would cost approximately 0.15 m/s over the OTM-359–OTM-360 optimization chain case. A single maneuver to achieve the T95 aimpoint

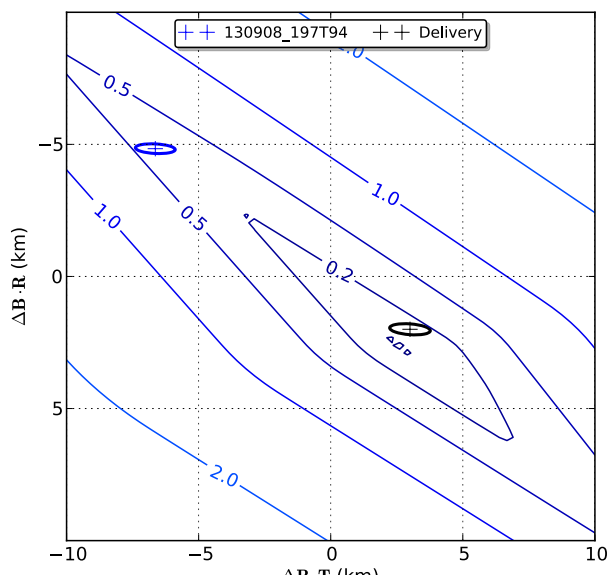


Figure 9: T94 Cost Contours (OTM-358)

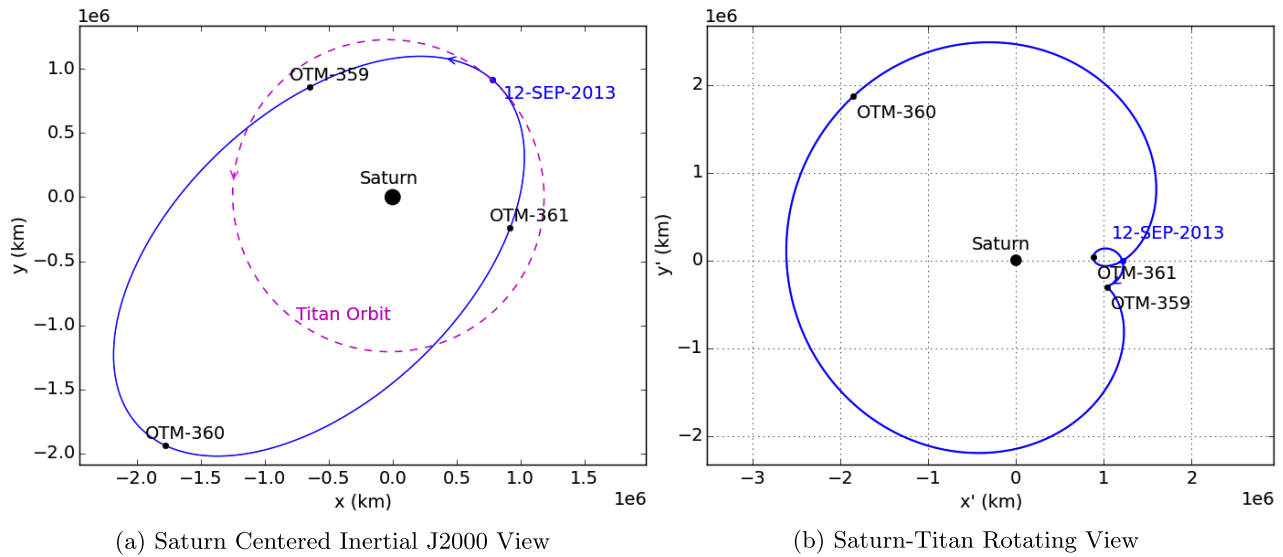


Figure 10: Cassini's 2:1 resonant trajectory from 12-Sep-2013 to 14-Oct-2013 as viewed from (a) inertial and (b) rotating reference frames.

would have resulted in a large RCS burn of 0.22 m/s via OTM-359 or 0.24 m/s via OTM-360. In the interest of saving hydrazine and to minimize the growth of OTM-360, the OTM-359–OTM-360 optimization chain approach was taken. OTM-360 was a required maneuver that would cost nearly 30 m/s if cancelled. Finally, OTM-361 was executed to preserve about 67 mm/s in downstream  $\Delta V$ .

### 3. Titan-95 to Titan-96: 3:1 Resonant Transfer

Cassini's 3:1 resonant trajectory from T95 on 14-Oct-2013 (blue dot) to T96 on 01-Dec-2013 is represented in Figure 11. The plot in Figure 11a depicts the trajectory as viewed from a Saturn-centered J2000 coordinate frame with Titan's orbit represented by the dotted magenta line. The locations of OTM-362, OTM-363, and OTM-364 are represented by the black dots along the transfer orbit. Figure 11b illustrates Cassini's transfer trajectory from T95 to T96 as viewed from a Saturn-Titan rotating coordinate frame.

The T95–T96 encounter is characterized by the cancellation of the cleanup maneuver, OTM-362. The decision of canceling OTM-362 was made based on the fact that the designed maneuver was too small for implementation ( $\Delta V = 7.7$  mm/s).

Additionally, there was virtually no downstream  $\Delta V$  penalty for canceling the maneuver, i.e., the cancellation cost was  $-5.9$  mm/s (a  $\Delta V$  savings, actually). The apoapsis maneuver, OTM-363, was performed, with a prohibitive downstream cost of more than 75 m/s if cancelled. Finally, the approach maneuver OTM-364 was required to avoid a cancellation cost of 0.74 m/s, but the initial design of this maneuver was too small to implement. T96 was modified by  $-0.25$  seconds to increase the OTM-364  $\Delta V$  to an executable size of 14.0 mm/s. Incidentally, this was the smallest RCS burn commanded at 8.2 mm/s, minus the 5.8 mm/s correction term for deadband-tightening  $\Delta V$  and an observed fixed-magnitude bias  $\Delta V$  in RCS burns. The amount to change the time of flight was determined using Figure 12 (see Shift 2 solution).

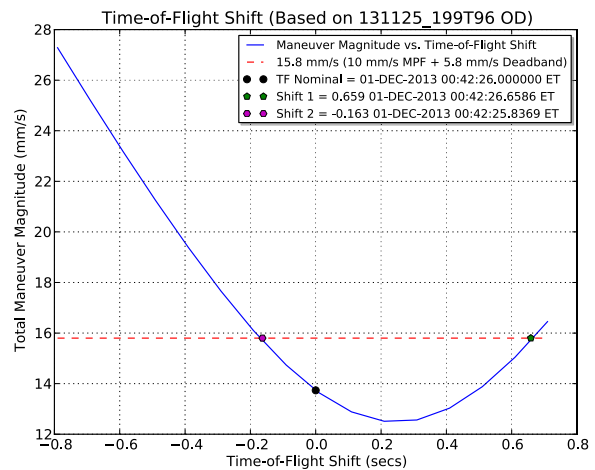


Figure 12: T96 Time-of-Flight Shift via OTM-364

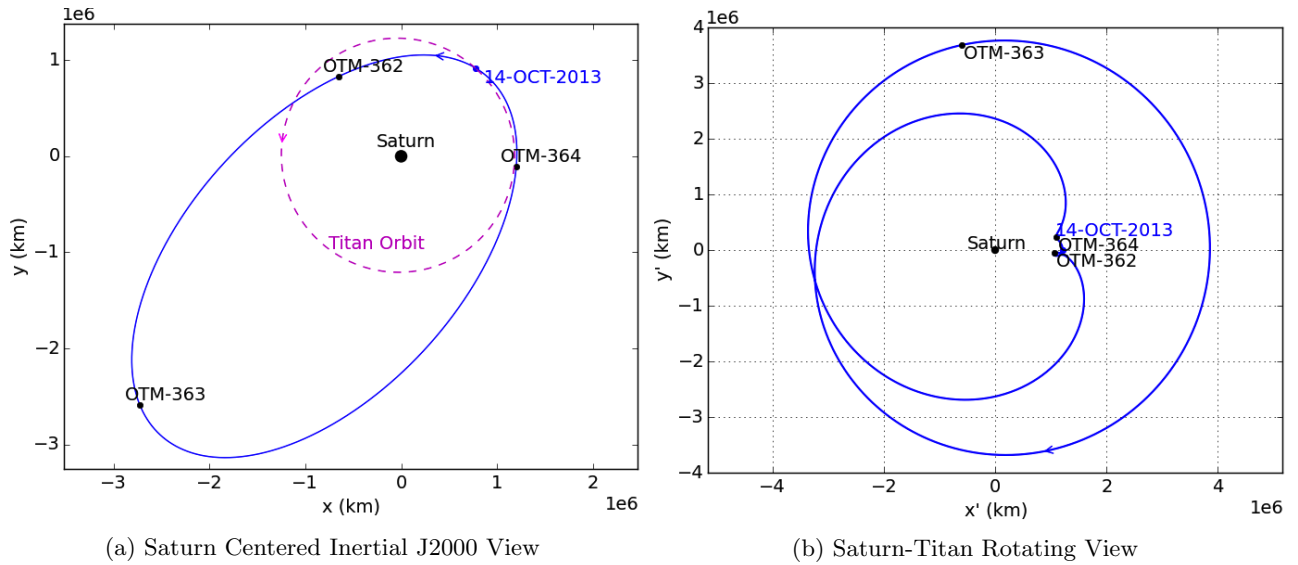


Figure 11: Cassini's 3:1 resonant trajectory from 14-Oct-2013 to 01-Dec-2013 as viewed from (a) inertial and (b) rotating reference frames.

#### 4. Titan-96 to Titan-100: 2:1 Resonant Transfers

The next four encounters, from T96 on 01-Dec-2013 to T100 on 07-Apr-2014, include same resonant ratio transfers. Cassini's 2:1 resonant trajectories are represented in Figure 13; views of the transfers from a Saturn-centered J2000 coordinate frame and a Saturn-Titan rotating coordinate frame appear in Figure 13a and Figure 13b, respectively. The locations of the 15 planned OTMs during these Titan flybys are labeled and represented by the black dots.

The cleanup maneuver after T96, OTM-365, was skipped as the  $\Delta V$  penalty for cancellation was reasonably small ( $\sim 52$  mm/s). The Project made the decision of canceling the maneuver based on the following three factors: (1) 26 mm/s of hydrazine would be saved, (2) a maneuver cycle reduced, and (3) the trajectory reconstruction would be more accurate. The subsequent apoapsis and approach maneuvers, OTM-366 and OTM-367, were performed nominally with no first time events. Surprisingly, OTM-367 was the largest RCS performed during the fourth year of the Solstice Mission at 0.115 m/s, the last RCS  $\Delta V$  this size in April 2013 w/ OTM-347.<sup>15</sup>

The maneuver targeting strategy for the next encounter, T97–T98, was slightly modified. Rather than applying a two-maneuver chain optimization scheme to design the two deterministic maneuvers in this encounter, the cleanup maneuver after the T97 flyby, OTM-368, was designed as a single maneuver targeting directly to the T98 flyby B-plane. Consequently, after implementation, OTM-369 was deemed unnecessary to achieve the B-plane target and, therefore, canceled. In fact, the deterministic savings achieved by performing OTM-369 instead of OTM-370 were deemed to be smaller than the statistical cost incurred from larger T98 flyby errors. Performing both OTM-369 and OTM-370 was not a viable option since the approach maneuver, OTM-370, would then consist primarily of a time-bias component. Finally, OTM-370 was performed nominally to prevent a downstream cost of more than 3 m/s.

The next three planned maneuvers, OTMs 371–373, were all implemented to achieve the targets at the T99 B-plane, mainly to assist the T100-T101 pi-transfer. To save more than 100 mm/s in downstream  $\Delta V$ , OTM-371 and OTM-372 were designed in an optimization chain with subsequent maneuvers. OTM-372 was a main engine burn of 1.7 m/s; if delayed to OTM-373, a  $\Delta V$  penalty of more than 55 m/s would result. Much of this cost was attributed to the T101 targeting maneuver OTM-378 which is essential in maintaining the T100-T101 pi-transfer. OTM-373 was performed as the final targeting maneuver to T99 to preserve 1.7 m/s downstream, half of which was reflected in the increased size of OTM-378.

After an accurate T99 flyby, it was determined that the cleanup maneuver, OTM-374, was unnecessary. Additionally, there were small  $\Delta V$  savings by canceling the maneuver. OTM-375 was executed as a small main engine burn (0.54 m/s) and uplinked early to move Cassini off an impacting trajectory with Titan.

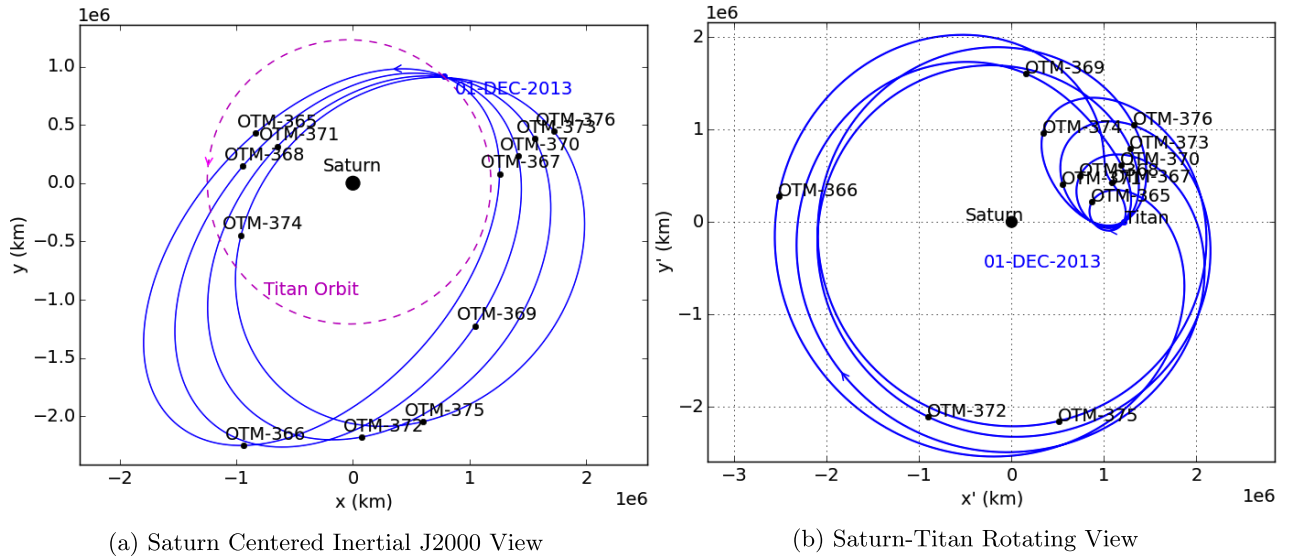


Figure 13: Cassini's 2:1 resonant trajectories from 01-Dec-2013 to 07-Apr-2014 as viewed from (a) inertial and (b) rotating reference frames.

Canceling OTM-375 and delaying to OTM-376 would have resulted in a downstream cost over 13 m/s. Finally, OTM-376 was implemented to correct a remaining  $\sim 13$  km from the T99 target which would translate into a 5.3 m/s cost.

5. Titan-100 to Titan-101:  $\pi$ -Transfer

The next targeted Titan flyby, T101, was achieved via a special case of a non-resonant transfer. In a non-resonant transfer, the time-of-flight is *not* an integer multiple of the gravity-assist body's orbit. The flybys, therefore, occur at different longitudes in Titan's orbit. Because the flybys of a non-resonant transfer do not occur at the same longitude, the spacecraft's orbit plane is constrained to be the same as the gravity-assist body's orbit plane. A  $\pi$ -transfer is a special case of a non-resonant transfer, where the time-of-flight of the transfer is  $m + 1/2$  times the period of Titan. The flybys of a  $\pi$ -transfer occur on either side of a line passing through Saturn, and thus, these transfers can also be inclined. This 40-day  $\pi$ -transfer changed the longitude of the T101 encounter by  $180^\circ$ .

Cassini's  $\pi$ -transfer from T100 on 07-Apr-2014 to T101 on 17-May-2014 is represented in Figure 15. Views of the 40-day non-resonant transfer from both a Saturn-centered J2000 coordinate frame and a Saturn-Titan rotating coordinate frame appear in Figure 15a and Figure 15b, respectively. The black dots on both Figures indicate the locations of the three planned OTMs targeting to T101. For reference, the blue arrow indicates the direction of motion.

Following the T100 encounter, OTM-378 and OTM-379 were designed in an optimization chain with subsequent maneuver to correct for the small T100 flyby miss. This strategy also saved over 100 mm/s over performing the correction entirely with OTM-378, which may have grown to nearly 0.2 m/s. OTM-378 was executed to complete the T101 targeting, reducing the downstream cost by nearly 1.4 m/s. OTM-379, the final maneuver opportunity for targeting T101, was too small to implement. By changing the B-plane aim-

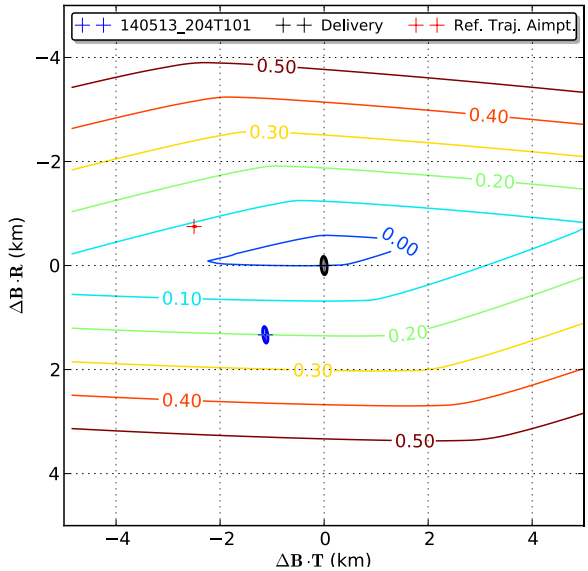


Figure 14: T101 Cost Contours (OTM-379)

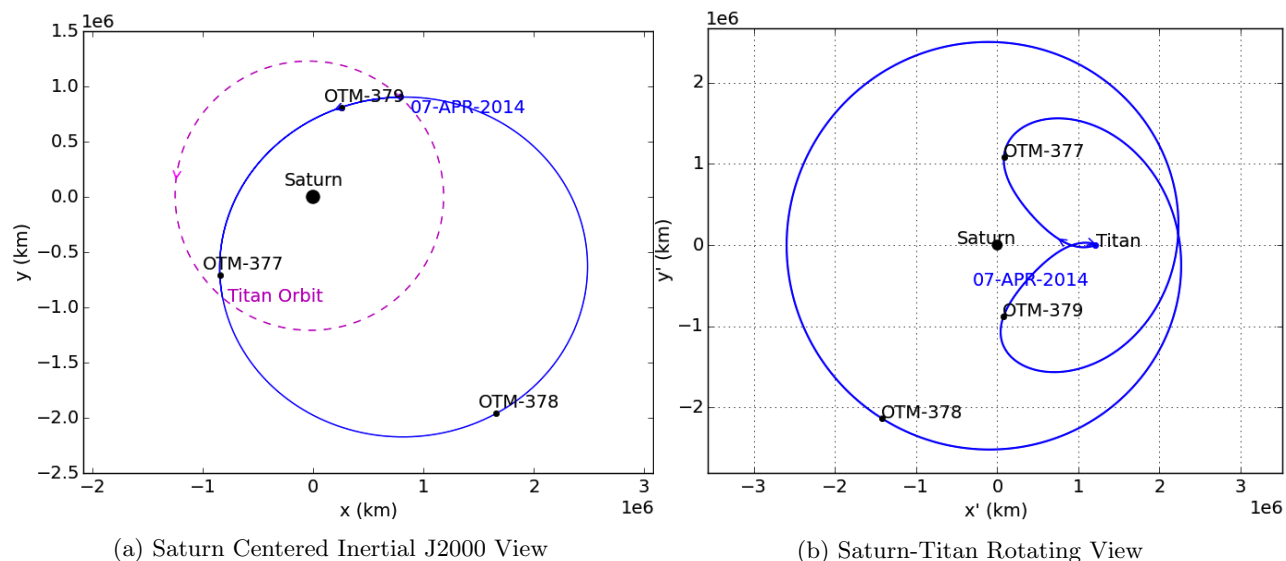


Figure 15: Cassini’s 40-day pi-transfer from 07-Apr-2014 to 17-May-2014 as viewed from (a) inertial and (b) rotating reference frames.

point by +0.75 km in  $\mathbf{B} \cdot \mathbf{R}$  and +2.5 km in  $\mathbf{B} \cdot \mathbf{T}$  (see Figure 14), not only was OTM-379 increased to an executable size, it also reduced the downstream cost by 120 mm/s. This would be the second time this type of B-plane targeting strategy would be taken to make a maneuver implementable, the first time with OTM-316.<sup>14</sup>

Pi-transfers are valuable from a science perspective since the orbit of spacecraft is altered exploiting Titan’s gravity to gain different perspectives on Saturn and achieve a wide variety of science objectives. That is, during a pi-transfer, Cassini flies by Titan at opposite sides of its orbit about Saturn and uses the moon’s gravity to change its orbital perspective on the ringed planet. However, pi-transfers are also interesting from a dynamical systems perspective since the transfer itself seems to be connecting two different periodic, resonant orbits with different flyby angles separated by 180°. For better visualization, Figure 16 depicts the orbits pre- and post- pi-transfer, that is, the two 2:1 resonant orbits between T99–T100 and T101–T102, respectively, as viewed from a Saturn-Titan rotating reference frame.

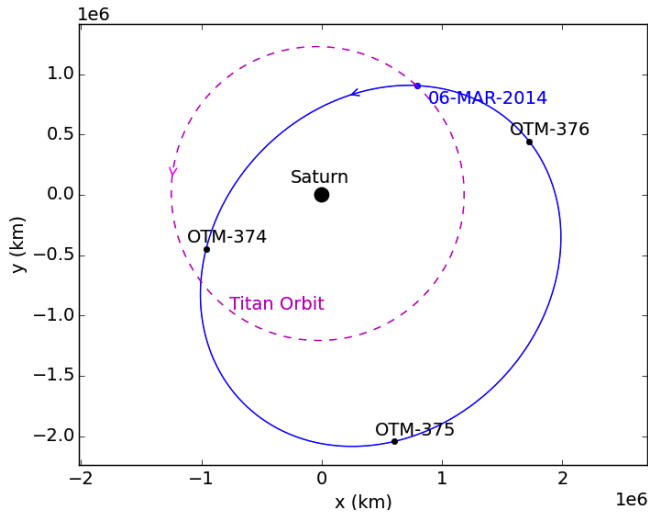
### 6. Titan-101 to Titan-102: 2:1 Resonant Transfer

Cassini’s 2:1 resonant trajectory from 17-May-2014 to 18-Jun-2014 is represented in Figure 16d, as viewed from a rotating reference frame. After the T101 flyby, OTM-380 was performed to correct for the small flyby errors, resulting in a cancelation of the subsequent apoapsis maneuver, OTM-381. Designing OTM-380 and OTM-381 together in an optimization chain with downstream maneuvers would have resulted in both maneuvers being too small to execute. Following the execution of OTM-380, OTM-381 became a small, non-implementable  $\Delta V$  with an insignificant cancelation cost. The approach maneuver to T102, OTM-382, was implemented nominally to preserve about 52 mm/s in projected downstream cost.

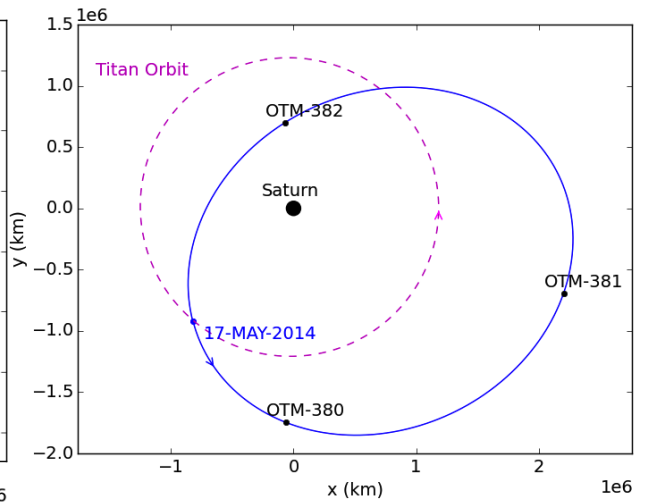
## C. Navigation Cost Analysis

To aid in understanding the Cassini tour navigation strategy, the maneuver performance per flyby is summarized in Table 5. This maneuver performance, represented by the navigation  $\Delta V$  cost per flyby (see last column), is evaluated by comparing the reconstructed  $\Delta V$  from each encounter span to the planned  $\Delta V$  from the reference trajectory (see shaded columns). The predicted  $\Delta V$  statistics per flyby are garnered from statistical analyses reported in Reference 25 and later updated in operations.

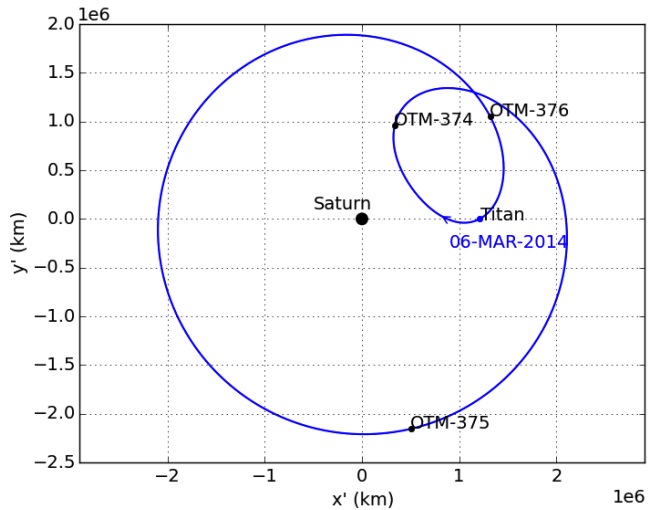
The average navigation  $\Delta V$  cost per flyby is summarized in Table 6. The cost between each encounter was not as evenly distributed prior to the Solstice Mission, as evidenced by the large standard deviation of nearly 1 m/s for the Equinox Mission reported in the table. With the majority of the maneuvers performed



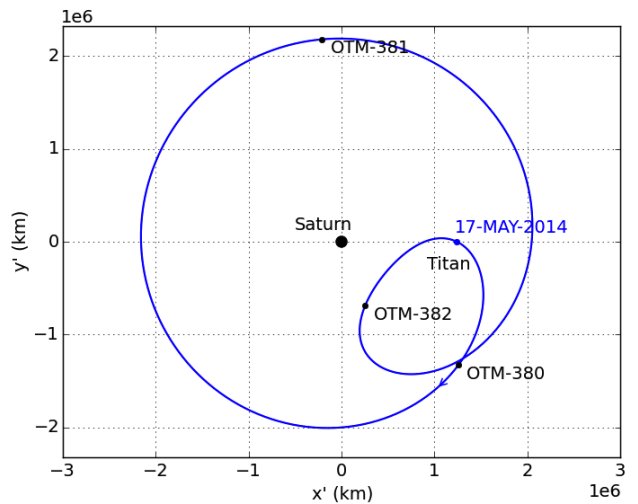
(a) Inertial J2000 Pre-Pi-Transfer 2:1 Resonant Orbit



(b) Inertial J2000 Post-Pi-Transfer 2:1 Resonant Orbit



(c) Rotating Pre-Pi-Transfer 2:1 Resonant Orbit



(d) Rotating Post-Pi-Transfer 2:1 Resonant Orbit

Figure 16: (a) Rotating frame view of Cassini's pre-pi-transfer trajectory from 06-Mar-2014 to 07-Apr-2014. (b) Rotating frame view of Cassini's post-pi-transfer trajectory from 17-May-2014 to 18-Jun-2014.

Table 5: Maneuver Performance per Encounter

Encounter Span	Ref. Traj.	Predicted $\Delta V$ Statistics			Design	Recon.	Navigation
	Det. $\Delta V$ (m/s)	Mean (m/s)	1- $\sigma$ (m/s)	90%* (m/s)	$\Delta V$ (m/s)	$\Delta V$ (m/s)	$\Delta V$ Cost <sup>†</sup> (m/s)
T92 – T93	2.409	3.068	0.551	3.818	2.591	2.589	<b>0.180</b>
T93 – T94	3.610	4.269	0.453	4.888	3.649	3.654	<b>0.044</b>
T94 – T95	0.074	0.350	0.213	0.653	0.123	0.122	<b>0.048</b>
T95 – T96	0.378	0.770	0.227	1.071	0.378	0.379	<b>0.001</b>
T96 – T97	0.399	0.805	0.337	1.258	0.501	0.495	<b>0.096</b>
T97 – T98	0.004	0.531	0.372	1.058	0.159	0.157	<b>0.153</b>
T98 – T99	1.718	1.951	0.127	2.127	1.796	1.795	<b>0.077</b>
T99 – T100	0.553	0.743	0.124	0.907	0.597	0.599	<b>0.046</b>
T100 – T101	0.002	0.405	0.325	0.860	0.096	0.093	<b>0.091</b>
T101 – T102 <sup>‡</sup>	0.003	0.162	0.129	0.323	0.047	0.049	0.045

\* Total  $\Delta V$  in encounter span will be less than or equal to this value with a 90% confidence level.

<sup>†</sup> Navigation  $\Delta V$  cost = reconstructed  $\Delta V$  – reference trajectory deterministic  $\Delta V$ . Note, the computed navigation costs are based on the raw numbers to avoid round-off errors.

<sup>‡</sup> Reported navigation cost is based on preliminary orbit determination estimates.

on RCS during the Solstice Mission, the average navigation cost so far has been less than half the average costs seen in the prior missions.

Table 6: Average Navigation  $\Delta V$  Cost per Encounter

Mission	Flyby Span	Number of Flybys	Navigation $\Delta V$ Cost	
			Average (m/s)	Std. Dev. (m/s)
Prime (7/2004 – 9/2008)	Ta – E4	54	0.324	0.594
Equinox (9/2008 – 9/2010)	E5 – T72	36	0.447	0.978
Solstice (9/2010 – 6/2014, First 4 Years)	T73 – T102	41	0.117	0.129

From Figure 17, it can be seen that from the start of the Solstice Mission, the upward Navigation cost trend had been curbed (see Reference 15 for more details).

#### IV. End-of-Mission Preview

The fourth year of Solstice Mission maneuver operations is marked by the low percentage of planned maneuvers canceled. This pattern, also seen during the third year of the Solstice Mission, is likely to continue as the Navigation Team strives to adhere to the reference trajectory. With mostly low Titan flybys through 2014 and 2015, this trend of fewer maneuver cancellations is expected to persist. A current main navigation strategy is to fly Cassini as close to the prescribed trajectory as possible in an effort to save propellant, particularly hydrazine. Hydrazine is the limiting factor for maneuvers. Maneuvers, as well as spacecraft pointing and wheel management cannot be accomplished via the main engine. Therefore, to reduce hydrazine consumption and prevent RCS thruster degradation, small main engine burns are now preferred over large RCS maneuvers, with the exception of approach maneuvers targeting low flyby altitudes.

Due to Planetary Protection requirements, before the spacecraft runs out of propellant, the possibility of future impact with any of the large icy moons, such as Enceladus, has to be precluded. After multiple studies were carried out, the option of culminating with Saturn impact after a series of short-period, highly inclined orbits was incorporated in the final phase of the Solstice Mission. As of January 2014, about xx m/s of bipropellant  $\Delta V$  are available for main engine maneuvers and approximately xx m/s of hydrazine  $\Delta V$  for RCS burns are expected to be available at end-of-mission (at the 90% confidence level), resulting in a total

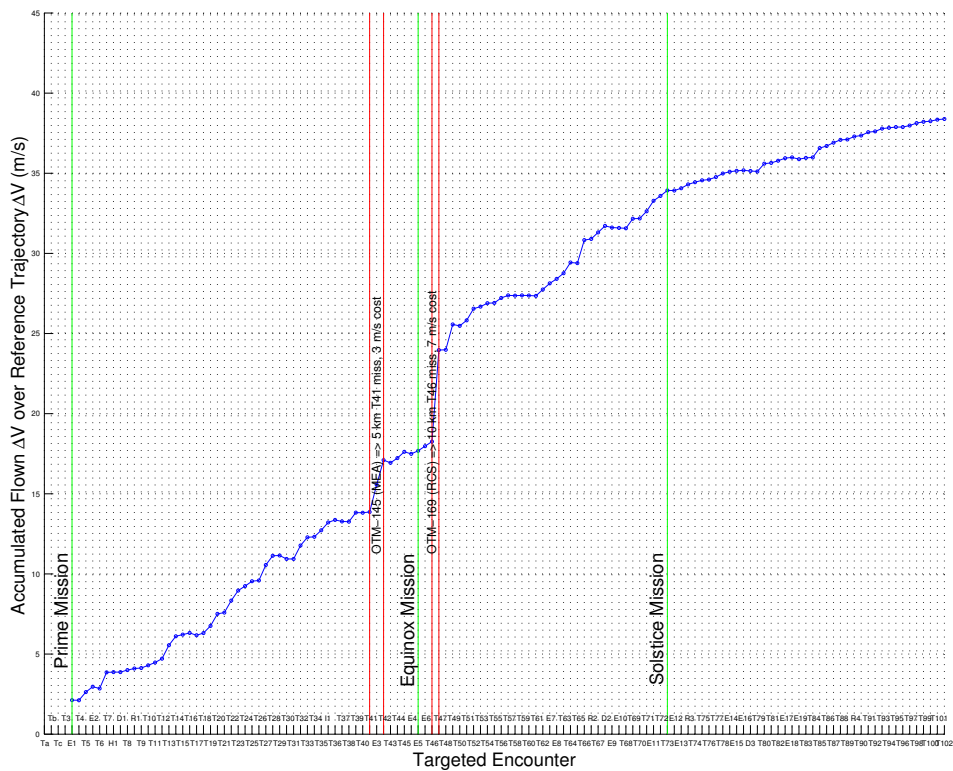


Figure 17: Accumulated Flown  $\Delta V$  Cost over Reference Trajectory  $\Delta V$

of xx m/s.<sup>26</sup> With this  $\Delta V$  margin and three more years for Cassini to fly the Saturn tour, it is vital that the Cassini Project continues to explore different maneuver strategies for preserving propellant.

## Acknowledgments

This research was carried out at the Jet Propulsion Laboratory, California Institute of Technology, under a contract with the National Aeronautics and Space Administration.

## References

- <sup>1</sup>“Cassini Navigation Plan,” Tech. Rep. 699-101 Update, JPL D-11621, NASA Jet Propulsion Laboratory, Pasadena, CA, July 1, 2003.
- <sup>2</sup>“Cassini Solstice Mission Navigation Plan,” Tech. Rep. 699-101 Update, JPL D-11621, NASA Jet Propulsion Laboratory, Pasadena, CA, February 3, 2010.
- <sup>3</sup>“Cassini Extended Mission Navigation Plan,” Tech. Rep. 699-101 Update, JPL D-11621, NASA Jet Propulsion Laboratory, Pasadena, CA, March 6, 2008.
- <sup>4</sup>Goodson, T. D., Gray, D. L., Hahn, Y., and Peralta, F., “Cassini Maneuver Experience: Launch and Early Cruise,” *AIAA Guidance, Navigation, & Control Conference*, AIAA Paper 98-4224, Boston, MA, August 10–12, 1998.
- <sup>5</sup>Goodson, T. D., Gray, D. L., Hahn, Y., and Peralta, F., “Cassini Maneuver Experience: Finishing Inner Cruise,” *AAS/AIAA Space Flight Mechanics Meeting*, AAS Paper 00-167, Clearwater, FL, January 23–26, 2000.
- <sup>6</sup>Goodson, T. D., Buffington, B. B., Hahn, Y., Strange, N. J., Wagner, S. V., and Wong, M. C., “Cassini-Huygens Maneuver Experience: Cruise and Arrival at Saturn,” *AAS/AIAA Astrodynamics Specialist Conference*, AAS Paper 05-286, Lake Tahoe, CA, August 7–11, 2005.
- <sup>7</sup>Wagner, S. V., Buffington, B. B., Goodson, T. D., Hahn, Y., Strange, N. J., and Wong, M. C., “Cassini-Huygens Maneuver Experience: First Year of Saturn Tour,” *AAS/AIAA Astrodynamics Specialist Conference*, AAS Paper 05-287, Lake Tahoe, CA, August 7–11, 2005.
- <sup>8</sup>Wagner, S. V., Gist, E. M., Goodson, T. D., Hahn, Y., Stumpf, P. W., and Williams, P. N., “Cassini-Huygens Maneuver Experience: Second Year of Saturn Tour,” *AIAA/AAS Astrodynamics Specialist Conference*, AIAA-2006-6663, Keystone, CO, August 21–24, 2006.

- <sup>9</sup>Williams, P. N., Gist, E. M., Goodson, T. D., Hahn, Y., Stumpf, P. W., and Wagner, S. V., “Cassini-Huygens Maneuver Experience: Third Year of Saturn Tour,” *AAS/AIAA Astrodynamics Specialist Conference*, AAS Paper 07-254, Mackinac Island, MI, August 19–23, 2007.
- <sup>10</sup>Goodson, T. D., Ballard, C. G., Gist, E. M., Hahn, Y., Stumpf, P. W., Wagner, S. V., and Williams, P. N., “Cassini Maneuver Experience: Ending the Prime Mission,” *AIAA/AAS Astrodynamics Specialist Conference*, AIAA-2008-6751, Honolulu, HI, August 18–21, 2008.
- <sup>11</sup>Gist, E. M., Ballard, C. G., Hahn, Y., Stumpf, P. W., Wagner, S. V., and Williams, P. N., “Cassini-Huygens Maneuver Experience: First Year of the Equinox Mission,” *AAS/AIAA Astrodynamics Specialist Conference*, AAS Paper 09-349, Pittsburgh, PA, August 9–13, 2009.
- <sup>12</sup>Ballard, C. G., Arrieta, J., Hahn, Y., Stumpf, P. W., Wagner, S. V., and Williams, P. N., “Cassini Maneuver Experience: Ending the Equinox Mission,” *AIAA/AAS Astrodynamics Specialist Conference*, AIAA-2010-8257, Toronto, Canada, August 2–5, 2010.
- <sup>13</sup>Wagner, S. V., Arrieta, J., Ballard, C. G., Hahn, Y., Stumpf, P. W., and Valerino, P. N., “Cassini Solstice Mission Maneuver Experience: Year One,” *AAS/AIAA Astrodynamics Specialist Conference*, AAS Paper 11-528, Girdwood, AK, July 31–August 4, 2011.
- <sup>14</sup>Arrieta, J., Ballard, C. G., Hahn, Y., Stumpf, P. W., Valerino, P. N., and Wagner, S. V., “Cassini Solstice Mission Maneuver Experience: Year Two,” *AIAA/AAS Astrodynamics Specialist Conference*, AIAA-2012-4433, Minneapolis, MN, August 13–16, 2012.
- <sup>15</sup>Wagner, S. V., Arrieta, J., Hahn, Y., Stumpf, P. W., Valerino, P. N., and Wong, M. C., “Cassini Solstice Mission Maneuver Experience: Year Three,” *AAS/AIAA Astrodynamics Specialist Conference*, AAS Paper 13-717, Hilton Head, SC, August 11–15, 2013.
- <sup>16</sup>Smith, J. and Buffington, B., “Overview of the Cassini Solstice Mission Trajectory,” *AAS/AIAA Astrodynamics Specialist Conference*, AAS Paper 09-351, Pittsburgh, PA, August 9–13, 2009.
- <sup>17</sup>Arrieta, J., “Diagrammatic Representation of Orbital Events,” NASA Jet Propulsion Laboratory, Pasadena, CA.
- <sup>18</sup>Williams, P. N., Gist, E. M., Goodson, T. D., Hahn, Y., Stumpf, P. W., and Wagner, S. V., “Orbit Control Operations for the Cassini-Huygens Mission,” *SpaceOps 2008 Conference*, AIAA-2008-3429, Heidelberg, Germany, May 12–16, 2008.
- <sup>19</sup>Kizner, W., “A Method of Describing Miss Distances for Lunar and Interplanetary Trajectories,” August 1, 1959.
- <sup>20</sup>Gates, C. R., “A Simplified Model of Midcourse Maneuver Execution Errors,” Tech. Rep. 32-504, NASA Jet Propulsion Laboratory, Pasadena, CA, October 15, 1963.
- <sup>21</sup>Wagner, S. V., “Maneuver Performance Assessment of the Cassini Spacecraft Through Execution-Error Modeling and Analysis,” *AAS/AIAA Space Flight Mechanics Meeting*, AAS Paper 14-390, Santa Fe, New Mexico, January 26–30, 2014.
- <sup>22</sup>Wagner, S. V. and Goodson, T. D., “Execution-Error Modeling and Analysis of the Cassini-Huygens Spacecraft Through 2007,” *AAS/AIAA Space Flight Mechanics Meeting*, AAS Paper 08-113, Galveston, TX, January 27–31, 2008.
- <sup>23</sup>C. D. Murray and S. F. Dermott, *Solar System Dynamics*, Cambridge University Press, Cambridge, Cambridge, United Kingdom, 1999.
- <sup>24</sup>Stumpf, P. W., Gist, E. M., Goodson, T. D., Hahn, Y., Wagner, S. V., and Williams, P. N., “Flyby Error Analysis Based on Contour Plots for the Cassini Tour,” *AIAA/AAS Astrodynamics Specialist Conference*, AIAA-2008-6749, Honolulu, HI, August 18–21, 2008.
- <sup>25</sup>Ballard, C. G. and Ionasescu, R., “Flight Path Control Design for the Cassini Solstice Mission,” *AAS/AIAA Astrodynamics Specialists Conference*, AAS Paper 11-530, Girdwood, AK, July 31–August 4, 2011.
- <sup>26</sup>Manor-Chapman, E., “Instrument and Spacecraft Consumables Status,” *Cassini Mission Planning Forum*, February 26, 2013.